# Novel Approach to Construct Realistic Magnetic Field Configuration in the Lower Solar Atmosphere

V. Fedun[1], F. A. Gent[2], G. Verth[2], S.J. Mumford[2], I. Giagkiozis[2,3], R. Erdélyi[2]

[1]SP$^2$RC, Space Systems Laboratory, Department of Automatic Control and Systems Engineering, University of Sheffield, Sheffield, S1 3JD, UK.
[2]SP$^2$RC, School of Mathematics and Statistics, University of Sheffield, Sheffield, S3 7RH, UK.
[3]Complex Optimization and Decision Making Laboratory, Department of Automatic Control and Systems Engineering, University of Sheffield, Sheffield, S1 3JD, UK.

## Abstract

Models of realistic magnetic field configurations, typical of the lower solar atmosphere, are analytically constructed in magneto-hydrostatic equilibrium. Systems incorporating open single and multiple flux tubes and closed magnetic loops can be combined to form magnetic structures that could even represent complex solar active regions.
The developed model successfully spans the Interface Region of the solar atmosphere, from the photosphere up to the solar corona across the challenging transition region, while retaining physically valid plasma pressure, density and magnetic flux distributions. Modelling magnetic structures can capture the main characteristics of solar intergranular lanes or active regions. HMI data can be used, as an initial magnetic field distribution, to construct a realistic magnetic field topology in 3D. The model includes a number of free parameters. Our aim is to apply this model as the background state to numerically study energy transport mechanisms from solar surface to corona.

## Simulations

Using a steady background with a single axisymmetric open magnetic flux tube, the system is perturbed and various modes of energy wave propogation from surface to atmosphere probed (see e.g. Fedun, Erdélyi & Shelyag, 2009, SolPhys, Mumford, Fedun & Erdélyi, 2014, ApJ, Shelyag, Fedun, Erdélyi, 2008, A&A and Vigeesh et. al, 2012, ApJ. In 3D these models are confined to the chromosphere. Physically consistent equilibria for both the chromosphere and corona is very challenging.

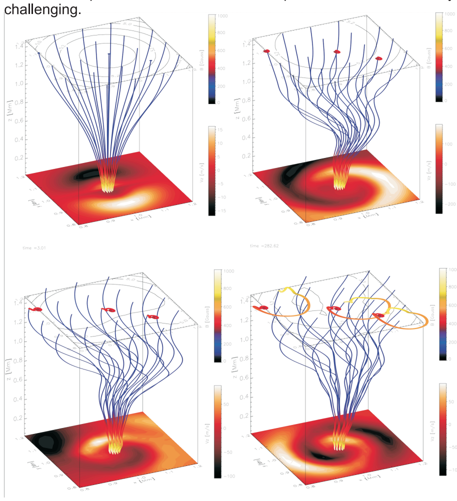

Three-dimensional snapshots of the MHD wave propagation in an open magnetic flux tube are shown. The thin multicolor curves represent the magnetic field lines. The lower and upper color bars correspond to the vertical velocity Vz at the level of the driver location and to the strength value of the magnetic field along the magnetic field lines, respectively. The black iso-contours of the magnetic field labeled by appropriate value of the strength of the magnetic field are shown in the top horizontal slice taken at height h = 1.4 Mm. At the bottom of each snapshot the horizontal cross-cut at the location of the swirl driver is shown. The 3D trajectory of the top ends of the three representative magnetic field lines are shown as colored thick curves.

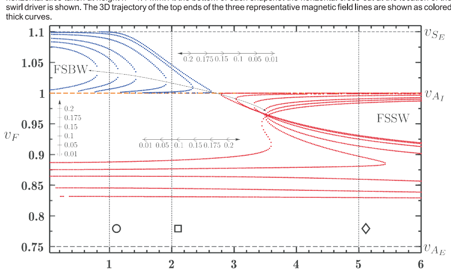


Solutions of the dispersion equation in presence of internal and external twist for a cool evacuated magnetic flux tube embedded in a dense environment ($\beta_i$<<1, $\beta_e$ >>1) with speed ordering $V_{Se} > V_{Ai} > V_{Ae} > V_{si}$.

## Magnetic twist

The presence of weak twist changes the character of axisymmetric modes in a significant way as seen in the figure below. Namely, while in the case with no magnetic twist the azimuthal component of the velocity perturbation is zero, in the case with twist this component is almost never zero. This effect is clearly seen, where the relative magnitude of the radial and azimuthal components of the velocity perturbation alternate periodically. Also, given that observations of Alfvén waves rely on the apparent absence of intensity (i.e. density) perturbations in conjunction with torsional motion, we suggest an alternative interpretation. Namely, observed waves that appear to be Alfénic in nature could actually be surface sausage waves (see right panel of the below figure), since due to the localised character of the density perturbation, this perturbation could be below the instrument resolution.

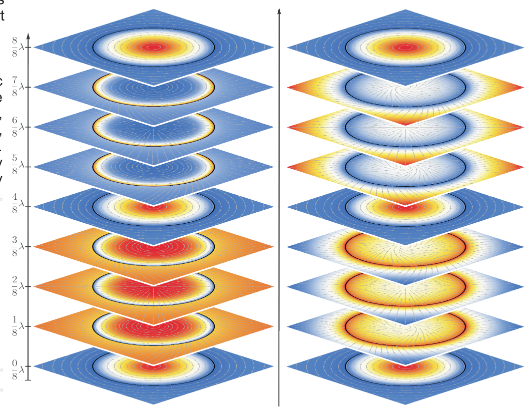

## Magnetohydrostatic equilibrium

Given the configuration for the steady background magnetic field $\boldsymbol{B}_b$, the background plasma pressure $p_b$ and density $\rho_b$ must adjust to satisfy the pressure balance,

$$\nabla p_b + \nabla\frac{|\boldsymbol{B}_b|}{2\mu_0} - \left(\frac{\boldsymbol{B}_b}{2\mu_0}\cdot\nabla\right)\boldsymbol{B}_b - \rho_b g\hat{\boldsymbol{R}} = \boldsymbol{0}, \quad (1)$$

$\mu_0$ magnetic vacuum permeabilty, $g$ gravitational acceleration.

## Single flux tube

For an $m^{th}$ flux tube, denoted $^m\boldsymbol{B}_b$, where for the single tube $m$=1, the magnetic field has the self-similar relations,

$$\begin{aligned} {}^mB_{bx} &= -{}^mS(x - {}^mx)B_{0z}\,{}^mG\,\frac{\partial B_{0z}}{\partial z}, \\ {}^mB_{by} &= -{}^mS(y - {}^my)B_{0z}\,{}^mG\,\frac{\partial B_{0z}}{\partial z}, \\ {}^mB_{bz} &= \quad {}^mS{B_{0z}}^2\,{}^mG\,, \end{aligned} \quad (2)$$

where ($^mx$, $^my$) locates surface longitude and latitude of the footpoint axis, and $z$ is the solar radius, with $z$=0 the radius of the photosphere. The sign of real $^mS$ determines polarity.

$$\begin{aligned} {}^mf &= {}^mrB_{0z}, \quad {}^mr = \sqrt{(x-{}^mx)^2+(y-{}^my)^2}, & (3) \\ B_{0z} &= b_{01}\exp\left(-\frac{z}{z_1}\right) + b_{02}\exp\left(-\frac{z}{z_2}\right), & (4) \\ {}^mG &= \frac{2\ell}{\sqrt{\pi}f_0}\exp\left(-\frac{{}^mf^2}{{f_0}^2}\right). & (5) \end{aligned}$$

Constants $z_1$, $z_2$, $b_{01}$ & $b_{02}$ fix flux tube expansion rates for the chromosphere and corona, and $f_0$ its thickness.

## Compatibility condition

A solution to Eq. (1) exists if the following conditions on the magnetic field are satisfied (see e.g. Gent, Fedun & Erdelyi, 2014, ApJ, Low, 1985, ApJ), which is the case for the single flux tube,

$$\frac{\partial B_x}{\partial y} = \frac{\partial B_y}{\partial x} \quad \text{and} \quad \frac{\partial B_z}{\partial y}\frac{\partial B_x}{\partial z} = \frac{\partial B_z}{\partial x}\frac{\partial B_y}{\partial z}. \quad (6)$$

## Multiple flux tubes

Multiple flux tubes may be specified by a background field,

$$\boldsymbol{B}_b = \sum_{m=1}^{N} {}^m\boldsymbol{B}_b$$

differing only by position ($^mx$, $^my$). Eq. (1) solves almost completely. A small part of the magnetic tension force, relating interaction between each flux tube pair, fails the latter condition in Eq. (6).
Equilibrium is maintained by including balancing forces in the momentum and energy equation of the form,

$$\boldsymbol{F}_{\rm bal} = \sum_{m,n=1|m\neq n}^{N} \frac{{}^nB_{bz}}{\mu_0}\frac{\partial\,{}^mB_{bx}}{\partial z}\hat{\boldsymbol{x}} + \frac{{}^nB_{bz}}{\mu_0}\frac{\partial\,{}^mB_{by}}{\partial z}\hat{\boldsymbol{y}} + 0\hat{\boldsymbol{z}}, \quad (7)$$

and solving a modified equation of pressure balance,

$$\nabla p_b + \nabla\frac{|\boldsymbol{B}_b|}{2\mu_0} - \left(\frac{\boldsymbol{B}_b}{2\mu_0}\cdot\nabla\right)\boldsymbol{B}_b - \rho_b g\hat{\boldsymbol{R}} + \boldsymbol{F}_{\rm bal} = \boldsymbol{0}. \quad (8)$$

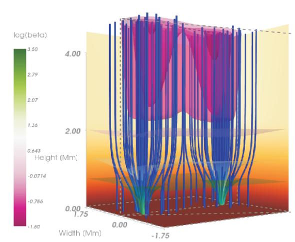

With the additional constraint that the solution to Eq. (8) must yield $p_b$ and $\rho_b$, and plasma temperatures, which are consistent with observation, various steady multiple flux tube configurations can be modelled.

Left, two pairs of flux tubes in 3D view show magnetic field lines (blue), plasma pressure (brown) and plasma-β iso-surfaces (purple - green). Right, is the 2D-slice of magnetic pressure.

## The modified MHD equations

Magnetic field, energy and density decompose into background and perturbed quantities,

$$\boldsymbol{B} = \boldsymbol{B}_b + \tilde{\boldsymbol{B}},\; e = e_b + \tilde{e} \text{ and } \rho = \rho_b + \tilde{\rho},$$

where the background does not evolve. The ideal MHD equations are modified to remove the $\boldsymbol{0}$ contribution from Eq. (8), and evolve the perturbed system. For the momentum equation,

$$\frac{\partial[(\rho_b+\tilde{\rho})u_i]}{\partial t} + \frac{\partial}{\partial x_j}\left[(\rho_b+\tilde{\rho})u_iu_j + \tilde{p}_T\right] - \frac{\partial}{\partial x_j}\left[\frac{\tilde{B}_iB_{bj} + B_{bi}\tilde{B}_j + \tilde{B}_i\tilde{B}_j}{\mu_0}\right] - F_{{\rm bal}_i} = \tilde{\rho}g_i, \quad (9)$$

in which $\boldsymbol{u}$ is the velocity and the total perturbed pressure,

$$\tilde{p}_T = (\gamma-1)\left[\tilde{e} - \frac{(\rho_b+\tilde{\rho})u_ju_j}{2}\right] - (\gamma-2)\left[\frac{\tilde{B}_jB_{bj}}{\mu_0} + \frac{\tilde{B}_j\tilde{B}_j}{2\mu_0}\right].$$

and similarly for the full ideal MHD system. Examples of applications include inter-granular lanes (below) and active regions, with a magnetic canopy (lower).